Water Research 93 (2016) 141–152

Contents lists available at ScienceDirect

Water Research

journal homepage: www.elsevier.com/locate/watres

Growth, microcystin-production and proteomic responses of *Microcystis aeruginosa* under long-term exposure to amoxicillin

Ying Liu*, Shi Chen, Jian Zhang, Baoyu Gao

Shandong Provincial Key Laboratory of Water Pollution Control and Resource Reuse, School of Environmental Science and Engineering, Shandong University, Jinan, 250100, PR China

ARTICLE INFO

Article history:
Received 25 September 2015
Received in revised form
17 January 2016
Accepted 30 January 2016
Available online 13 February 2016

Keywords:
Combined pollution
Antibiotic toxicity
Semi-continuous culture
Photosynthesis activity
Two-dimensional electrophoresis
Protein–protein interaction network

ABSTRACT

Ecological risk of antibiotics due to the induction of antibiotic-resistant bacteria has been widely investigated, while studies on the hazard of antibiotic contaminants *via* the regulation of cyanobacteria were still limited. This study focused on the long-term action effect and mechanism of amoxicillin (a broadly used antibiotic) in *Microcystis aeruginosa* at environmentally relevant concentrations through 30 days of semi-continuous culture. Amoxicillin stimulated the photosynthesis activity and the production of microcystins, and interaction of differential proteins under amoxicillin exposure further manifested the close correlation between the two processes. D1 protein, ATP synthase subunits alpha and beta, enolase, triosephosphate isomerase and phosphoglycerate kinase were candidate target positions of amoxicillin in *M. aeruginosa* under long-term exposure. Amoxicillin affected the cellular biosynthesis process and the metabolism of carbohydrate and nucleoside phosphate according to the proteomic responses. Under exposure to amoxicillin, stimulated growth rate at the beginning phase and increased production and release of microcystins during the whole exposure period would lead to a higher contamination of *M. aeruginosa* cells and microcystins, indicating that amoxicillin was harmful to aquatic environments through the promotion of cyanobacterial bloom.

1. Introduction

Antibiotics are widely used in agriculture, human medicine and veterinary, and are consequently released into aquatic environments through agricultural runoff and the discharge of hospital and urban wastewater, either directly or after treatment (Rodriguez-Mozaz et al., 2015). Though most antibiotics have short half-lives, the continuous production and discharge of antibiotics still lead to a pseudo-persistent contamination (Kümmerer, 2009). Studies of the ecological risk of antibiotic contaminants mainly focus on the induction of antibiotic-resistant bacteria, which are normally considered as the most significant adverse effect of antibiotics (Pruden, 2014).

It is noteworthy that cyanobacteria is also an important phylum of bacteria, though they obtain energy through photosynthesis rather than catabolism (Stanier and Cohen-Bazire, 1977). Cyanobacteria are principal primary producers in aquatic ecosystems under their normal growth conditions, while excessive growth of cyanobacteria can lead to harmful blooms, especially for toxic strains that produce cyanotoxins (Graham et al., 2010). Recent studies observed that antibiotics may promote the bloom of cyanobacteria at low concentrations while were toxic to cyanobacteria at high concentrations (González-Pleiter et al., 2013; Pomati et al., 2004), indicating that antibiotic contaminants have the potential to affect the aquatic ecosystem through the regulation of cyanobacteria bloom.

Currently observed effects of antibiotics on cyanobacteria were mainly obtained from short-term exposure tests through batch culture, and the duration of the tests was normally no more than 7 days (Halling-Sørensen, 2000). However, cyanobacteria in the actual aquatic environment are supposed to be chronically exposed to antibiotics due to their pseudo-persistent contamination (Kümmerer, 2009). Long-term environmental impact of antibiotics *via* the regulation of cyanobacterial growth and cyanotoxin-production at their currently detected concentrations would be more meaningful but has not yet been revealed. A continuous/semi-continuous algal toxicity test is suggested by ecotoxicologists as an alternative approach to evaluate the effect of toxicants on phytoplanktons (Hiriart-Baer et al., 2006), which is also a

* Corresponding author.
E-mail address: liuying2010@sdu.edu.cn (Y. Liu).

http://dx.doi.org/10.1016/j.watres.2016.01.060
0043-1354/

feasible route to study the long-term effect of antibiotic contaminants in cyanobacteria.

Besides, the action mechanism of antibiotic contaminants in cyanobacteria remain unclear. Though previous studies suggested that reactive oxygen species, antioxidant enzymes, polysaccharides and several functional genes are potential biomarkers for antibiotics (Qian et al., 2012; Wan et al., 2015), responses to antibiotics on the overall level of certain intracellular components, such as proteome and genome, have not been reported. Since proteins participate in almost all the physiological functions, proteomic approaches have been successfully applied in cyanobacteria to understand their responses to various environmental stresses, such as N/P starvation, high light, heat shock, and heavy metals (Castielli et al., 2009; Mehta et al., 2014). Proteomic approaches make it possible to quickly screen target proteins (which controls the action of exogenous chemicals in the organism and induces responses of downstream proteins) from the whole proteome by comparing the proteomic profiles between exposed and un-exposed organisms (Bandow et al., 2003), but have not been used to interpret the action mechanism of antibiotics in cyanobacteria.

Amoxicillin is an broadly used antibiotic with high activity against bacteria, and previous studies of our group found that amoxicillin stimulated the growth of *Microcystis aeruginosa* (a model species of cyanobacteria) and the production of microcystins (MCs) at environmentally relevant concentrations of $\leq$600 ng/L through a 7-day short-term exposure test (Liu et al., 2015). In order to further explore the long-term action effect and mechanism of typical antibiotics in cyanobacteria, *M. aeruginosa* in this study was exposed to amoxicillin for 30 days through a semi-continuous culture, and the alterations in growth rate, photosynthesis activity, MC-production and release as well as the responses of the whole proteome were examined.

2. Materials and methods

2.1. Semi-continuous culture of M. aeruginosa

M. aeruginosa NIES-843 was supplied by the Freshwater Algae Culture Collection at the Institute of Hydrobiology (Wuhan, China). Experimental apparatuses and BG11 medium used for the culture of *M. aeruginosa* were sterilized by autoclave at 121 °C for 20 min before use. The cyanobacterium was pre-cultured for two weeks in BG11 medium at 25 ± 1 °C under a 16:8 light: dark cycle provided by cool white fluorescent lights at an intensity of 40 μmol photons/($m^2 \cdot s$). After pre-cultivation, cyanobacterial cells at the exponential phase were collected by centrifugation (4000 g, 4 °C, 5 min) and used as inoculums for the amoxicillin-exposure test at an initial cell density of 4×10^5 cells/mL. Two exposure concentrations, 100 ng/L and 300 ng/L, were tested. For each test concentration, 500 mL Erlenmeyer flasks, each containing 200 mL of sterile BG11 medium, were spiked with different volumes of amoxicillin stock solution, each in triplicate. Amoxicillin was purchased from Sigma–Aldrich, Inc. (Shanghai, China), and the stock solution was prepared in methanol and stored at −20 °C prior to use. The final concentrations of methanol in the test media were below 0.01% (v/v). Each test medium was first cultured for 3 days, and then a certain volume of the test medium (with cyanobacterial cells) was removed from the flask and replaced by fresh medium (without cyanobacterial cells) every day. The removed medium was then used to analyze the cellular and proteomic responses in *M. aeruginosa*. The dilution rate was defined as D = F/V, where F was the replaced volume every day and V was the total medium volume in each flask. During the semi-continuous culture, the growth rate of *M. aeruginosa* was calculated every day according to a previous study (Liu et al., 2012), and the dilution rate was adjusted every day to keep equal to the growth rate. Amoxicillin was replenished regularly to maintain the test concentrations deviating within an acceptable range (from −9% to +11%) compared with their nominal values. Three flasks containing BG11 media spiked with 0.01% (v/v) methanol and without amoxicillin were prepared as the solvent control and cultured in the same procedure as amoxicillin-exposed groups. The semi-continuous culture of *M. aeruginosa* lasted for 30 days. A student's t test was used to determine the difference in the growth rate between each amoxicillin-exposed group and the solvent control at each day.

2.2. Analysis of cellular responses

Photosynthetic responses in *M. aeruginosa* was analyzed with a PhytoPAM fluorescence monitoring system (Walz, Germany) according to a previous study (Wang et al., 2010). The cyanobacterial cells were dark-adapted for 15 min, and then the minimum fluorescence (F_0) and the maximum fluorescence (F_m) were measured under a low light intensity and a saturating light pulse, respectively. The maximum photochemical quantum yield of photosystem II (PSII) was calculated as $F_v/F_m=(F_m-F_0)/F_m$. The rapid light curve (RLC) indicating the electron transport responses to increasing irradiance was then plotted, and the maximum relative electron transport rate ($rETR_{max}$) was calculated according to the relative value of the plateau phase in RLC.

Three most frequently detected MCs, MC-LR, MC-RR and MC-YR were selected as target MCs (Gupta et al., 2003). Culture medium and cyanobacterial cells were separated from each other through a Whatman GF/B filtration membrane (1 μm pore size) in order to separately measure the extracellular (C_{ex}) and intracellular (C_{in}) concentrations of MCs. The culture medium was extracted with Oasis HLB cartridges, and the cyanobacterial cells were subjected to ultrasonic-assisted extraction followed by Oasis HLB cartridge cleanup process. The extracts were measured with a Agilent 1200 series liquid chromatograph coupled with an Agilent series 6410B triple quadrupole mass spectrometer (Liu et al., 2015). The MC-production amount (fg per cell) was defined as the sum of C_{ex} and C_{in} divided by the cell density of *M. aeruginosa*. Release of MCs was indicated by the percentage of extracellular MCs in the total MC-production amount.

2.3. Analysis of proteomic responses

Proteomic responses were analyzed at the last day of amoxicillin-exposure at a low test concentration of 100 ng/L. A certain volume of the test medium was sampled from each flask according to the cell density, in order to obtain 1×10^9 of cyanobacterial cells, and divided into two technical replicates. The cyanobacterial cells were further collected by centrifugation, washed twice with Milli-Q water, extracted with a FOCUS™ Plant Proteome kit (G-Biosciences, USA) and finally purified with a Perfect-FOCUS™ kit following the protocol manuals. The protein content in the purified extract was determined with a Bio-Rad DC Protein Assay kit. The purified proteome was visualized by two-dimensional electrophoresis (2-DE) and Bio-Rad SYPRO Ruby staining. Six (3 biological replicates × 2 technical replicates) gels were prepared for the amoxicillin-exposed group and the solvent control for the quantitative analysis of proteome. Differentially expressed proteins with normalized fold change of $\geq$2.0 were identified by the Bio-Rad PDQuest 8.0 software (Chen et al., 2015). Spots of differentially expressed proteins were excised from gels, digested with trypsin, alkylated, desalted and then subjected to a AB SCIEX 5800-MALDI-TOF/TOF mass spectrometry (Franc et al., 2013; Franco et al., 2015; Guarino et al., 2014; He et al., 2013). The generated peak lists of the tryptic peptide masses were searched with MASCOT 2.2 (Matrix

Science, UK) against the database of *M. aeruginosa* from UniProt (updated on 2015/05/12). The whole procedure of 2-DE, mass spectrometry analysis and database searching were described in detail in the Supplementary Materials.

Annotation of Gene Ontology (GO) terms were conducted with AmiGO2 (http://amigo.geneontology.org/amigo). Pathway enrichment analysis and functional clustering of GO biological processes were performed using the online program DAVID (http://david.abcc.ncifcrf.gov/tools.jsp) according to Huang et al. (2009a, 2009b). The interaction network of differentially expressed proteins was constructed according to the STRING database (version 10.0, http://string-db.org) and then visualized using Cytoscape v2.8.2. The ClusterONE plugin of Cytoscape was used to identify functional modules with highly interconnected proteins ($p < 0.05$) among the protein–protein interaction network.

3. Results

3.1. Cellular responses to amoxicillin

Significant stimulation effect of amoxicillin ($p < 0.05$) on the growth of *M. aeruginosa* was observed since the second day of exposure and lasted for 14 and 10 days at test concentrations of 100 ng/L and 300 ng/L, respectively (Fig. 1). After that, no significant difference ($p > 0.05$) was observed in the growth rate between the control and each amoxicillin-exposed group. Different from the growth rate, the production and release of MCs in amoxicillin-exposed groups were higher than that in the control during the whole exposure period. Similar to the responses of MCs, F_v/F_m and rETRmax values in *M. aeruginosa* also increased under amoxicillin-exposure. The F_v/F_m value indicates the fraction of absorbed energy used for photochemistry in the total energy at a specific time, while the rETRmax value indicates the maximum photosynthetic capacity. This result suggested that amoxicillin enhanced the photosynthetic activity of *M. aeruginosa* at environmentally relevant concentrations.

3.2. Proteomic responses to amoxicillin

In order to further explore the long-term action mechanism of amoxicillin, the protein expression pattern of *M. aeruginosa* under exposure to amoxicillin was compared with the control. The lower test concentration (100 ng/L) group, which was more close to the low contamination level of amoxicillin in aquatic environments, was selected as the target group. A total of 207 protein spots were visualized in the master gel of the control (Fig. 2a), while the spot numbers in the amoxicillin-exposed group (Fig. 2b) was 210. After 30 days of exposure to 100 ng/L of amoxicillin, 37 proteins were up-regulated while 30 proteins were down-regulated, among which 35 number of up-regulated proteins and 27 number of down-regulated proteins were successfully identified by mass spectrometry (Table 1). The identified proteins were involved in six biological processes according to the GO annotation, including biological regulation, cellular process, response to stimulus, localization, metabolic process and signalling. The up-regulated proteins were more than the down-regulated ones, suggesting that the physiological activities in *M. aeruginosa* were stimulated to develop an inducible defence mechanism against the environmental stress caused by amoxicillin. Differentially expressed proteins were separately categorized into 61 biological processes and further clustered into 4 biological process groups (Table 2). Enrichment analysis of KEGG pathway indicated that three pathways, photosynthesis, carbon fixation in photosynthetic organisms and glycolysis/gluconeogenesis, were significantly enriched ($p < 0.05$) in *M. aeruginosa* exposed to amoxicillin (Table 3).

According to the protein–protein interaction analysis, 59 out of 62 differentially expressed proteins participated in 344 pairs of protein–protein interaction (Fig. 3). Though the interaction network was not yet validated by cellular responses observed in this study, the interconnection information among these proteins can facilitate the screening of target protein from amoxicillin-induced differentially expressed proteins (Andreani and Guerois, 2014). The degree of a node (protein) in the interaction network (indicated by different colors in Fig. 3) is the number of connections that it has to other nodes (proteins). Highly interconnected proteins with high degrees are supposed to play important roles in response to amoxicillin. In the interaction network, ten proteins with interconnection degrees higher than 21 were observed, including ATP synthase subunit alpha (atpA), enolase (eno), 10 kDa chaperonin (groS), Elongation factor Tu (tuf), Triosephosphate isomerase (tim), ATP synthase beta subunit (atpD), superoxide dismutase (sodB), glutamine synthetase (glnA), phosphoglycerate kinase (pgk) and thioredoxin peroxidase (MAE_35830). The protein–protein interaction network contained 3 significantly enriched ($p < 0.05$) functional modules (Fig. 4), in which proteins interconnected more closely with proteins within the module rather than with proteins outside the module (Dittrich et al., 2008). According to the annotation results, the first module containing 30 proteins was mainly related to the carbohydrate metabolic process group and the nucleoside phosphate metabolic process group (Table 2). The other two modules indicated a close interconnection between microcystin synthetase (mcyB) and photosynthesis-related proteins (Table 2).

4. Discussion

4.1. Hormesis effects of amoxicillin in M. aeruginosa

Antibiotic contaminants were found to cause hormesis effect in bacteria and plants at concentrations below toxic threshold (Migliore et al., 2010). In this study, hormesis effect of amoxicillin was also observed in the cyanobacterium *M. aeruginosa.* Firstly, photosynthesis activity was stimulated by amoxicillin at test concentrations of 100 and 300 ng/L during the whole exposure period, which were much lower than the toxic threshold of 6.88 μg/L (Liu et al., 2015). Photosynthesis works as the first step of energy production in *M. aeruginosa* by capturing solar energy and converting into chemical energy and biopolymers. And then, the stimulated photosynthesis activity coupled to increased energy production excited another two energy-consuming hormetic responses, the growth of *M. aeruginosa* and the production of MCs. Similar to the responses of photosynthesis activity, the MC-production amount increased during the whole exposure period. But the increased growth rate lasted for less than 15 days. The longer time duration suggested that the MC-production process was more adaptive to low exposure dose of amoxicillin and may be more effective in consuming the energy produced by photosynthesis, in comparison with the growth process.

The protein–protein interaction module illustrated by Fig. 4b further verified the close correlation between MC-production and photosynthesis. In this module, microcystin synthetase (mcyB) significantly interconnected ($p < 0.05$) with three PSII proteins (psbA, psb28 and psbO), two PSI proteins (psaB and psaC), one carbon fixation protein (cbbL), three photosynthetic pigments (apcB, pcA and pcB) and one photosynthesis-related electron transfer protein (fdx). Besides, previous studies suggested that MC-production was a defense response to various environmental stressers (Babica et al., 2006). This protein–protein interaction module also presented a significant interaction ($p < 0.05$) between microcystin synthetase (mcyB) and the universal stress protein

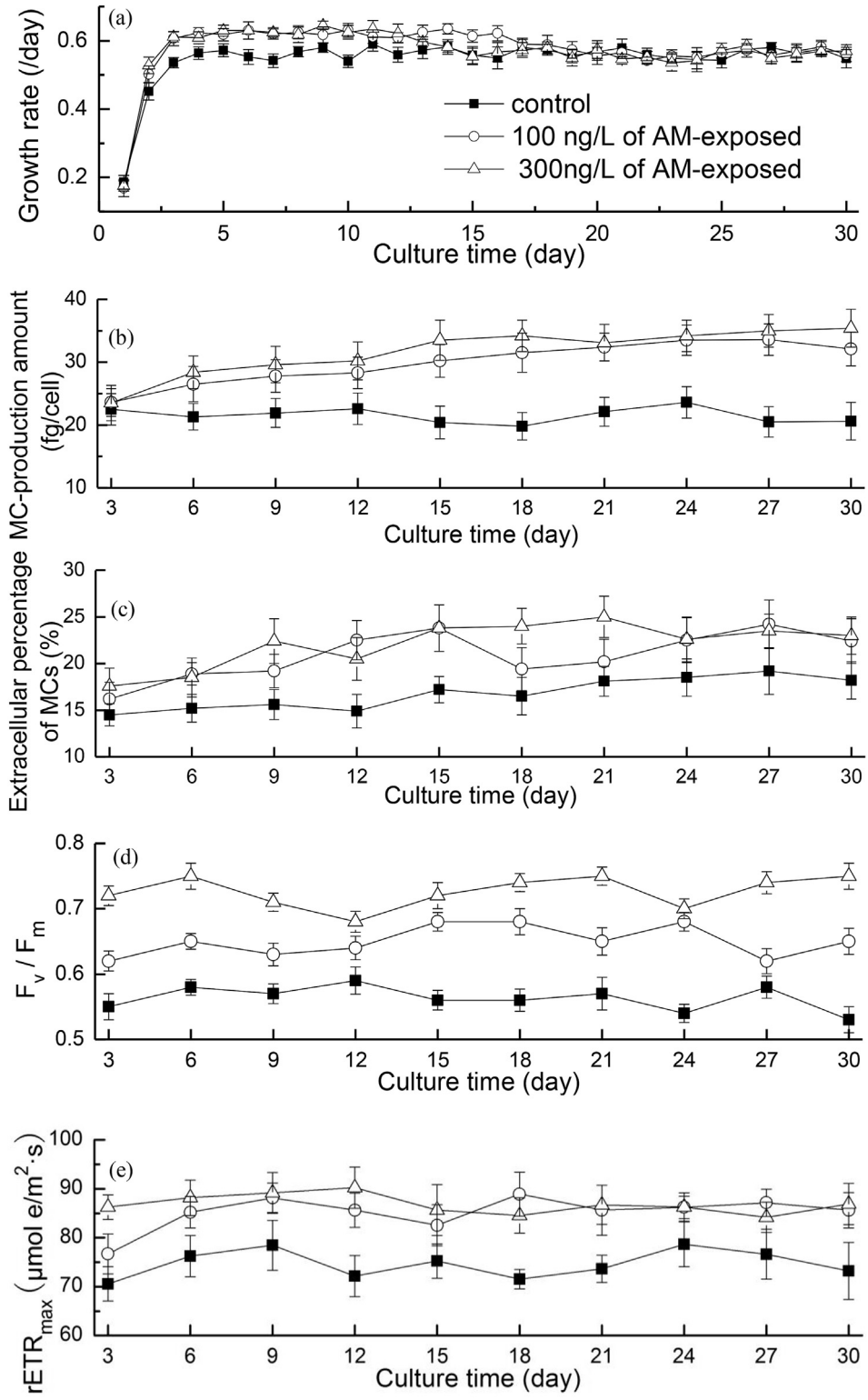

Fig. 1. Effect of amoxicillin on (a) the growth rate, (b) the MC-production amount, (c) the release of MCs, (d) the Fv/Fm value and (e) the rETRmax value of *M. aeruginosa* during the 30 days of exposure. Mean and standard deviation of three replicates are shown.

(MAE_48380) *via* the mediation of photosynthesis-related proteins. This result provided a direct evidence for a role of MCs in stress response to amoxicillin exposure. Photosynthesis-related proteins also mediated the correlation between microcystin synthetase (mcyB) and beta-lactamase-like protein (MAE_60380). The up-regulated expression of beta-lactamase-like protein (MAE_60380) was a specific stress response to amoxicillin, which could break the beta-lactam ring and inactivate amoxicillin (Pumirat et al., 2009). This result indicated that the two stress response processes were closely coupled with each other (Graham et al., 2010). The

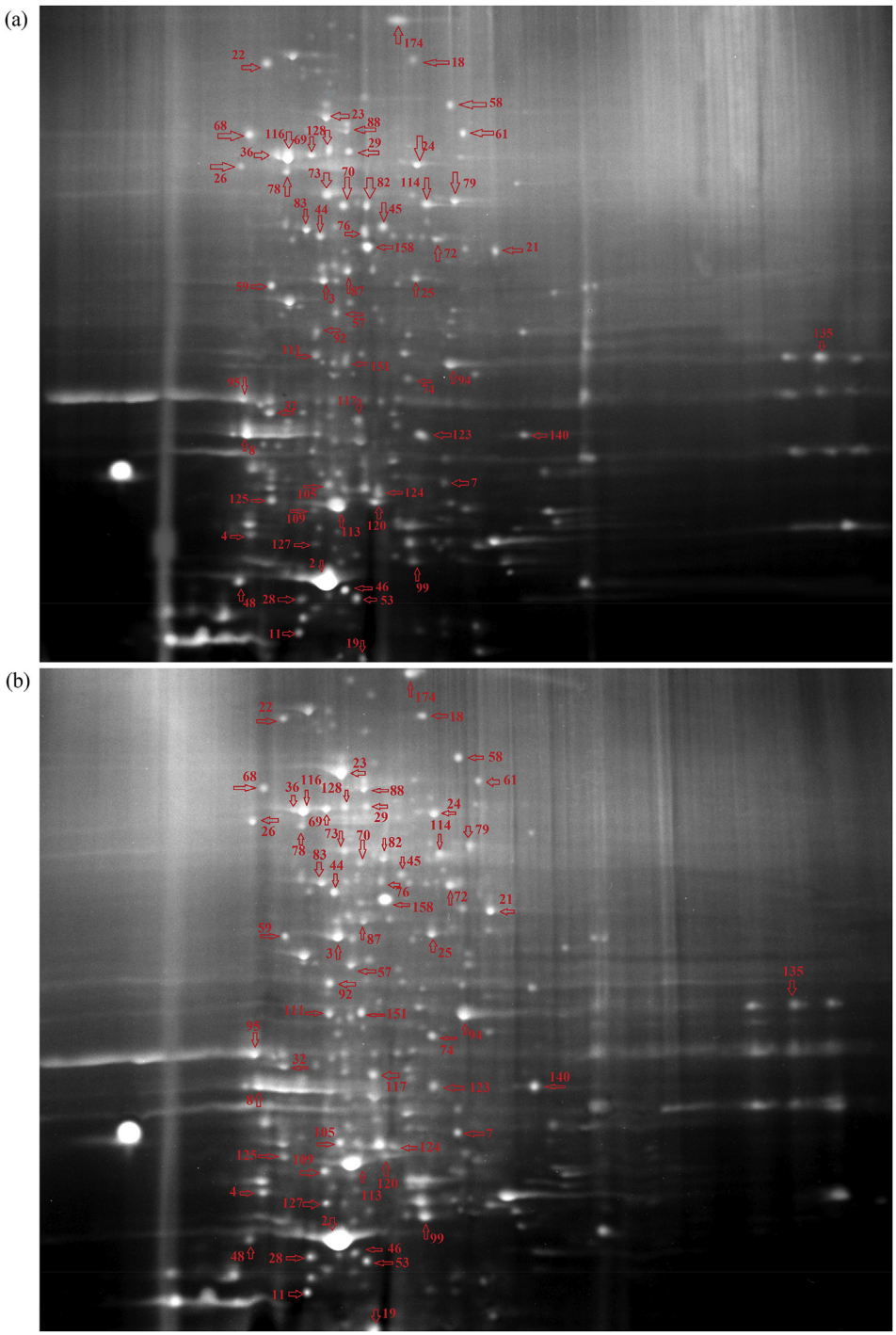

Fig. 2. 2-DE proteomic maps of *M. aeruginosa* after staining with SYPRO Ruby, including (a) the control and (b) *M. aeruginosa* exposed to 100 ng/L of amoxicillin for 30 days. Differentially expressed protein spots are further submitted to 5800-MALDI-TOF/TOF mass spectrometry. Successfully identified proteins are marked by different spot numbers, and the identified results are shown in Table 1.

protein–protein interaction (Fig. 4c) also suggested an potential interconnection among microcystin synthetase (mcyB), a transcription regulator binding to the promoter regions of the mcy gene cluster (ntcA), a nitrogen metabolism-related protein (nirA), a protein folding-related protein (MAE_13090) and a proteolysis-related protein (ctpA). Although MCs are nonribosomally synthesized peptides consisting of non-proteinogenic amino acids, this result suggested a possible connection between MC-production and protein metabolism.

Compared with the control, amoxicillin-treated *M. aeruginosa* released more MCs into the culture medium during the whole exposure period. Up-regulation of protein-export membrane protein and outer membrane efflux protein (Table 1) may facilitate the export of MCs with a cyclic heptapeptide structure. The ability of amoxicillin to break the cell wall may be another explanation for the stimulated release of MCs (Horii et al., 2002). Due to the exponential growth of *M. aeruginosa*, though the increased growth rate did not last until the end of the exposure, the final cell density

Table 1
The identified results of differentially expressed proteins in *M. aeruginosa* exposed to 100 ng/L of amoxicillin for 30 days. All the identified results except four proteins belong to *M. aeruginosa* NIES-843. The identified results of proteins numbered 3, 7, 26 and 72 belong to other species of *M. aeruginosa* and are marked in the brackets.

Spot number	UniProt ASNo.[a]	Protein name	Protein symbols	Theoretical MW/pI	Protein score/% confidence		Fold change
					MS	MS/MS	
GO Term: Biological regulation							
140	B0JRG0	Global nitrogen regulator Ycf28	ntcA	25206/6.92	125/100	98/100	2.25
GO Term: Cellular process							
11	B0JUI1	10 kDa chaperonin	groS	10729/5.11	204/100	158/100	2.24
23	B0JWI3	Ferredoxin-nitrite reductase	nirA	57077/5.46	154/100	85/99.89	2.37
29	B0JY25	Serine/threonine protein kinase like	MAE_52410	47118/5.62	162/100	83/100	0.45
44	B0JT86	Phosphoglycerate kinase	pgk	42640/5.11	165/100	98/100	2.36
53	B0JR76	Ferredoxin	fdx	13751/5.92	121/99.9	64/98.4	2.15
73	B0JSE0	Elongation factor Tu	tuf	44918/5.29	346/100	118/100	0.40
83	B0JTU3	Peptidyl-prolyl cis-trans isomerase	MAE_13090	40886/5.14	394/100	66/99.99	0.46
95	B0JN66	Protein grpE	grpE	26992/4.60	305/100	111/100	2.23
109	B0JUS6	Inorganic pyrophosphatase	ppa	18846/4.77	81/99.94	59/99.85	2.18
114	B0JWW0	Adenosylhomocysteinase	ahcY	45991/5.54	309/100	163/100	0.42
123	B0JFQ9	Imidazole glycerol phosphate synthase subunit HisH	hisH	23011/6.34	220/100	137/100	0.45
128	B0JU75	Two-component sensor histidine kinase	MAE_14410	46612/5.14	147/100	96/100	0.44
GO Term: Response to stimulus							
94	B0JVR7	Universal stress protein	MAE_48380	31446/6.64	305/100	107/100	2.36
105	B0JNH5	Thioredoxin peroxidase	MAE_35830	21916/4.70	85/99.96	75/99.62	2.05
113	B0JGF5	Superoxide dismutase	sodB	21847/4.96	375/100	102/100	2.24
124	B0JSA1	Two-component response regulator	MAE_42370	21099/6.34	251/100	87/100	0.44
GO Term: Localization							
57	B0JP76	Protein-export membrane proteinSecF	secF	34253/5.50	128/100	88/100	2.08
69	B0JUA7	Outer membrane efflux protein	MAE_14730	56435/5.21	676/100	121/100	2.34
70	B0JNV7	Polysaccharide export protein	MAE_37150	43827/5.47	340/100	107/100	0.45
76	B0JL32	Sodium-dependent bicarbonate transporter	MAE_62090	39838/5.49	118/100	72/98.7	0.44
GO Term: Metabolic process							
2	B0JHB6	Phycocyanin alpha subunit	cpcA1/pcA	17516/5.82	167/100	120/99.99	2.07
3	Q83UY7	Microcystin synthetase (*M. aeruginosa*)	mcyB	34958/5.92	88/99.2	72/99.2	2.32
4	B0JUG3	Pentapeptide repeat containing protein	MAE_45890	18036/4.36	167/100	76/100	2.13
7	I4H2F0	Phycobiliprotein beta chain (*M. aeruginosa* PCC 9806)	apcD	21799/6.61	71/98.88	60/98.20	2.08
8	B0JR79	O-methyltransferase	MAE_41260	24338/5.1	152/100	78/100	0.43
18	B0JTU4	Probable glycosyl transferase	MAE_13100	69156/5.99	241/100	104/100	2.14
19	B0JJ37	Photosystem I iron-sulfur center	psaC	8842/5.65	532/100	101/100	2.40
21	B0JWQ2	Chorismate synthase	aroC	39805/6.56	149/100	76/100	2.07
22	B0JUD1	Transketolase	MAE_14970	72232/5.45	111/99.90	60/99.80	0.41
24	B0JVL8	RuBisCO large chain	rbcL/cbbL	52544/6.04	121/100	92/100	2.06
25	B0JN21	Serine protease	MAE_03630	38792/6.33	169/100	88/100	2.15
26	H6VNP2	Microcystin synthetase (*M. aeruginosa* PCC7806)	mcyA	47893/4.70	85/98.80	68/98.50	2.25
28	B0JGJ5	Photosystem II reaction center Psb28 protein	psb28	12724/5.08	139/100	79/100	2.32
32	B0JSQ7	Triosephosphate isomerase	tpi/tim	25339/5.11	243/100	120/100	0.44
36	B0JXC2	Glutamine synthetase	glnA	53053/5.08	566/100	182/100	0.41
45	B0JNV4	Predicted pyridoxal dependent aminotransferase	MAE_37120	41339/5.59	390/100	98/100	0.42
46	B0JHT4	Nucleoside diphosphate kinase	ndk	16472/5.60	244/100	72/100	0.36
48	B0JRQ1	ATP-binding protein	MAE_09790	17100/4.34	140/100	94/100	0.37
58	B0JK06	Beta-lactamase-like protein	MAE_60380	61559/6.09	151/100	96/100	2.18
59	B0JPI1	Oxygen-dependent coproporphyrinogen-III oxidase	hemF	36806/5.54	141/100	81/100	0.46
61	B0JVE7	Glucose-6-phosphate isomerase	pgi	58113/5.81	124/100	96/100	0.38
68	B0JFM7	ATP synthase beta subunit	atpD	51614/4.87	770/100	120/100	0.48
72	I4HZ53	12-oxophytodienoate reductase 3 (*M. aeruginosa* PCC 9808)	OPR	41009/5.87	157/100	105/100	2.28
74	B0JLC0	Amino acid transport system ATP-binding protein	MAE_62970	27643/5.85	427/100	147/100	2.15
78	B0JMP6	Enolase	eno	46543/4.92	202/100	95/100	0.44
79	B0JLP6	Carboxyl-terminal processing protease	ctpA	45037/5.61	265/100	122/100	0.40
82	B0JUD0	3-oxoacyl-[acyl-carrier-protein] synthase II	MAE_14960	43646/5.80	572/100	130/100	0.35
87	B0JLP5	Fructose-bisphosphate aldolase class II	fbaA	38952/5.40	710/100	89/100	0.37
88	B0JUK0	Glutathione reductase	MAE_46260	49115/5.62	168/100	82/100	2.07
92	B0JJZ9	Cysteine synthase	cysK	34371/5.31	380/100	98/100	2.11
99	B0JRU8	Allophycocyanin beta subunit	apcB	17202/6.25	291/100	98/100	2.75
111	B0JTE4	Photosystem II manganese-stabilizing polypeptide	psbO	29877/4.67	467/100	137/100	2.13
116	B0JWV1	ATP synthase subunit alpha	atpA	53979/5.02	154/100	87/100	0.47
117	B0JWU0	PHA-specific acetoacetyl-CoA reductase	phaB	25190/5.66	164/100	112/100	2.27
120	B0JWV0	ATP synthase subunit delta	atpH	19629/6.34	348/100	77/100	0.35
127	B0JHB5	Phycocyanin beta subunit	cpcB1/pcB	18164/5.12	87/99.98	75/99.95	2.25
135	B0JP65	L-asparaginase II	MAE_05540	34614/8.43	452/100	140/100	0.48
151	B0JV73	Glutathione S-transferase	MAE_15850	29375/4.99	148/100	85/100	2.20
158	B0JIS8	Photosystem II protein D1	psbA	39715/5.38	125/100	88/100	2.32
174	B0JUY1	Photosystem I P700 chlorophyll a apoprotein A2	psaB	82332/6.58	112/100	76/100	2.19
GO Term: Signalling							
125	B0JM82	Putative chemotaxis protein	MAE_33450	19520/4.34	206/100	107/100	0.45

[a] Accession number.

Table 2
Clustering results of GO biological processes for differentially expressed proteins in *M. aeruginosa* exposed to 100 ng/L of amoxicillin for 30 days according to the online program DAVID.

Related process group	Enrichment score	Biological processes	Count	P value	Proteins
Photosynthesis and stress response	4.93	GO:0006091, generation of precursor metabolites and energy	18	3.6×10^{-10}	B0JWV1, B0JFM7, B0JWV0, B0JMP6, B0JVE7, B0JRU8, B0JHB5, B0JHB6, B0JLP5, B0JT86, B0JUY1, B0JJ37, B0JIS8, B0JSQ7
		GO:0015979, photosynthesis	13	3.7×10^{-6}	B0JRU8, B0JHB5, B0JHB6, B0JTE4, B0JUY1, B0JJ37, B0JGJ5, B0JIS8, B0JVL8
		GO:0009636, response to toxin	5	3.9×10^{-6}	B0JIS8
		GO:0009635, response to herbicide	5	3.9×10^{-6}	B0JIS8
		GO:0022900, electron transport chain	10	1.8×10^{-5}	B0JRU8, B0JHB5, B0JHB6, B0JUY1, B0JJ37, B0JIS8
		GO:0009772, photosynthetic electron transport in photosystem II	5	5.1×10^{-5}	B0JIS8
		GO:0055114, oxidation reduction	16	3.2×10^{-4}	B0JPI1, B0JRU8, B0JWI3, B0JHB5, B0JHB6, B0JUK0, B0JWU0, B0JUY1, B0JJ37, B0JIS8, B0JVL8, B0JGF5
		GO:0009767, photosynthetic electron transport chain	5	3.3×10^{-4}	B0JIS8
		GO:0019684, photosynthesis, light reaction	5	2.2×10^{-3}	B0JIS8
Carbohydrate metabolic process	2.19	GO:0006096, glycolysis	5	8.4×10^{-4}	B0JMP6, B0JVE7, B0JLP5, B0JT86, B0JSQ7
		GO:0006007, glucose catabolic process	5	3.2×10^{-3}	B0JMP6, B0JVE7, B0JLP5, B0JT86, B0JSQ7
		GO:0019320, hexose catabolic process	5	3.2×10^{-3}	B0JMP6, B0JVE7, B0JLP5, B0JT86, B0JSQ7
		GO:0046365, monosaccharide catabolic process	5	3.8×10^{-3}	B0JMP6, B0JVE7, B0JLP5, B0JT86, B0JSQ7
		GO:0046164, alcohol catabolic process	5	4.6×10^{-3}	B0JMP6, B0JVE7, B0JLP5, B0JT86, B0JSQ7
		GO:0044275, cellular carbohydrate catabolic process	5	5.3×10^{-3}	B0JMP6, B0JVE7, B0JLP5, B0JT86, B0JSQ7
		GO:0006006, glucose metabolic process	5	0.013	B0JMP6, B0JVE7, B0JLP5, B0JT86, B0JSQ7
		GO:0016052, carbohydrate catabolic process	5	0.013	B0JMP6, B0JVE7, B0JLP5, B0JT86, B0JSQ7
		GO:0019318, hexose metabolic process	5	0.021	B0JMP6, B0JVE7, B0JLP5, B0JT86, B0JSQ7
		GO:0005996, monosaccharide metabolic process	5	0.038	B0JMP6, B0JVE7, B0JLP5, B0JT86, B0JSQ7
Nucleoside phosphate metabolic process	1.14	GO:0055085, transmembrane transport	4	9.6×10^{-3}	B0JWV1, B0JFM7, B0JWV0, B0JP76
		GO:0009141, nucleoside triphosphate metabolic process	3	0.019	B0JWV1, B0JFM7, B0JWV0, B0JHT4
		GO:0009142, nucleoside triphosphate biosynthetic process	4	0.019	B0JWV1, B0JFM7, B0JWV0, B0JHT4
		GO:0009144, purine nucleoside triphosphate metabolic process	4	0.019	B0JWV1, B0JFM7, B0JWV0, B0JHT4
		GO:0009145, purine nucleoside triphosphate biosynthetic process	4	0.019	B0JWV1, B0JFM7, B0JWV0, B0JHT4
		GO:0009199, ribonucleoside triphosphate metabolic process	4	0.019	B0JWV1, B0JFM7, B0JWV0, B0JHT4
		GO:0009205, purine ribonucleoside triphosphate metabolic process	4	0.019	B0JWV1, B0JFM7, B0JWV0, B0JHT4
		GO:0009201, ribonucleoside triphosphate biosynthetic process	4	0.019	B0JWV1, B0JFM7, B0JWV0, B0JHT4
		GO:0009206, purine ribonucleoside triphosphate biosynthetic process	4	0.019	B0JWV1, B0JFM7, B0JWV0, B0JHT4
		GO:0015985, energy coupled proton transport, down electrochemical gradient	3	0.029	B0JWV1, B0JFM7, B0JWV0
		GO:0015986, ATP synthesis coupled proton transport	3	0.029	B0JWV1, B0JFM7, B0JWV0
		GO:0034220, ion transmembrane transport	3	0.029	B0JWV1, B0JFM7, B0JWV0
		GO:0006818, hydrogen transport	3	0.036	B0JWV1, B0JFM7, B0JWV0
		GO:0015992, proton transport	3	0.036	B0JWV1, B0JFM7, B0JWV0
		GO:0009152, purine ribonucleotide biosynthetic process	4	0.062	B0JWV1, B0JFM7, B0JWV0, B0JHT4
		GO:0009150, purine ribonucleotide metabolic process	4	0.062	B0JWV1, B0JFM7, B0JWV0, B0JHT4
		GO:0009259, ribonucleotide metabolic process	4	0.078	B0JWV1, B0JFM7, B0JWV0, B0JHT4
		GO:0009260, ribonucleotide biosynthetic process	4	0.078	B0JWV1, B0JFM7, B0JWV0, B0JHT4
		GO:0006164, purine nucleotide biosynthetic process	4	0.084	B0JWV1, B0JFM7, B0JWV0, B0JHT4

(*continued on next page*)

Table 2 (*continued*)

Related process group	Enrichment score	Biological processes	Count	P value	Proteins
		GO:0006163, purine nucleotide metabolic process	4	0.09	B0JWV1, B0JFM7, B0JWV0, B0JHT4
		GO:0006754, ATP biosynthetic process	3	0.1	B0JWV1, B0JFM7, B0JWV0
		GO:0046034, ATP metabolic process	3	0.1	B0JWV1, B0JFM7, B0JWV0
		GO:0006119, oxidative phosphorylation	3	0.17	B0JWV1, B0JFM7, B0JWV0
		GO:0015672, monovalent inorganic cation transport	3	0.19	B0JWV1, B0JFM7, B0JWV0
		GO:0009165, nucleotide biosynthetic process	4	0.21	B0JWV1, B0JFM7, B0JWV0, B0JHT4
		GO:0006793, phosphorus metabolic process	5	0.25	B0JWV1, B0JFM7, B0JWV0, B0JUS6, B0JU75
		GO:0006796, phosphate-containing compound metabolic process	5	0.25	B0JWV1, B0JFM7, B0JWV0, B0JUS6, B0JU75
		GO:0034654, nucleobase, nucleoside, nucleotide and nucleic acid biosynthetic process	4	0.3	B0JWV1, B0JFM7, B0JWV0, B0JHT4
		GO:0034404, nucleobase, nucleoside and nucleotide biosynthetic process	4	0.3	B0JWV1, B0JFM7, B0JWV0, B0JHT4
		GO:0044271, nitrogen compound biosynthetic process	9	0.33	B0JWV1, B0JFM7, B0JWV0, B0JWQ2, B0JJZ9, B0JXC2, B0JFQ9, B0JPI1, B0JHT4
		GO:0016310, phosphorylation	4	0.44	B0JWV1, B0JFM7, B0JWV0, B0JU75
		GO:0006812, cation transport	3	0.46	B0JWV1, B0JFM7, B0JWV0
		GO:0006811, ion transport	3	0.75	B0JWV1, B0JFM7, B0JWV0
Cellular biosynthetic process	0.42	GO:0044271, nitrogen compound biosynthetic process	9	0.33	B0JWV1, B0JFM7, B0JWV0, B0JWQ2, B0JJZ9, B0JXC2, B0JFQ9, B0JPI1, B0JHT4
		GO:0046394, carboxylic acid biosynthetic process	5	0.35	B0JWQ2, B0JJZ9, B0JXC2, B0JFQ9, B0JUD0
		GO:0016053, organic acid biosynthetic process	5	0.35	B0JWQ2, B0JJZ9, B0JXC2, B0JFQ9, B0JUD0
		GO:0008652, cellular amino acid biosynthetic process	4	0.42	B0JWQ2, B0JJZ9, B0JXC2, B0JFQ9
		GO:0009309, amine biosynthetic process	4	0.44	B0JWQ2, B0JJZ9, B0JXC2, B0JFQ9
Unculstered terms	NA[a]	GO:0018298, protein-chromophore linkage	4	0.012	B0JRU8, B0JHB5, B0JHB6, B0JUY1
		GO:0006457, protein folding	3	0.076	B0JUI1, B0JTU3, B0JN66
		GO:0016051, carbohydrate biosynthetic process	3	0.93	B0JVE7, B0JVL8, B0JSQ7
		GO:0051186, cofactor metabolic process	3	1	B0JPI1, B0JUK0, B0JSQ7

a: not avialable.

Table 3
Significantly enriched KEGG pathways ($p < 0.05$) and mapped proteins in 100 ng/L of amoxicillin-exposed group according to the online program DAVID.

Pathways	Count	P value	Proteins
Mar00195, Photosynthesis	13	2.9×10^{-6}	B0JWV1, B0JFM7, B0JWV0, B0JR76, B0JTE4, B0JUY1, B0JJ37, B0JGJ5, B0JIS8
Mar00710, Carbon fixation in photosynthetic organisms	5	0.014	B0JUD1, B0JLP5, B0JT86, B0JVL8, B0JSQ7
Mar00010, Glycolysis/Gluconeogenesis	5	0.046	B0JMP6, B0JVE7, B0JLP5, B0JT86, B0JSQ7

in the amoxicillin contaminated environment would still be much higher than that in the uncontaminated environment. Taking the increased production and release of MCs into account, co-existing amoxicillin would definitely increase the hazard of *M. aeruginosa*. The test concentrations of this study were below the upper contamination level of amoxicillin (622 ng/L) in aquatic environment (Zuccato et al., 2010), indicating that disturbance of ecological balance by amoxicillin through the regulation of cyanobacteria has already become an innegligible issue.

4.2. Action mechanism of amoxicillin in *M. aeruginosa*

After 30 days of exposure, two stress response proteins, universal stress protein and 10 kDa chaperonin were triggered by amoxicillin. The up-regulation of these two proteins were observed to regulate gene expression and protein folding in bacteria under various environmental stresses, including antibiotic exposure (Bangera et al., 2015). The up-regulation of superoxide dismutase suggested that amoxicillin generated reactive oxygen species (ROS) in *M. aeruginosa* and caused oxidative stress (Ni et al., 2015). Generation of ROS triggered the detoxification process. One phase I detoxification enzymes (thioredoxin peroxidase) and three phase II detoxification enzymes (glutathione S-transferase, glutathione reductase and probable glycosyl transferase) were up-regulated by amoxicillin. Though the detoxification process participated in scavenging ROS, down-regulation of elongation factor Tu suggested that amoxicillin finally caused oxidative damage in *M. aeruginosa* after 30 days of exposure (Zhang et al., 2012).

Both pathway enrichment analysis and functional clustering analysis manifested that photosynthesis was an important pathway/process in response to amoxicillin under long-term exposure. The first biological process group obtained by functional clustering analysis (Table 2) manifested the close correlation among photosynthesis, energy production and stress response to amoxicillin. The reaction center of PSII, D1 protein (psbA), played the most important role in this group, which was involved in all of the nine biological processes. Besides, PSI P700 chlorophyll a apoprotein A2 (psaB) and PSI iron-sulfur center (psaC) were also essential proteins in this group, which were involved in four biological processes (photosynthesis, generation of precursor

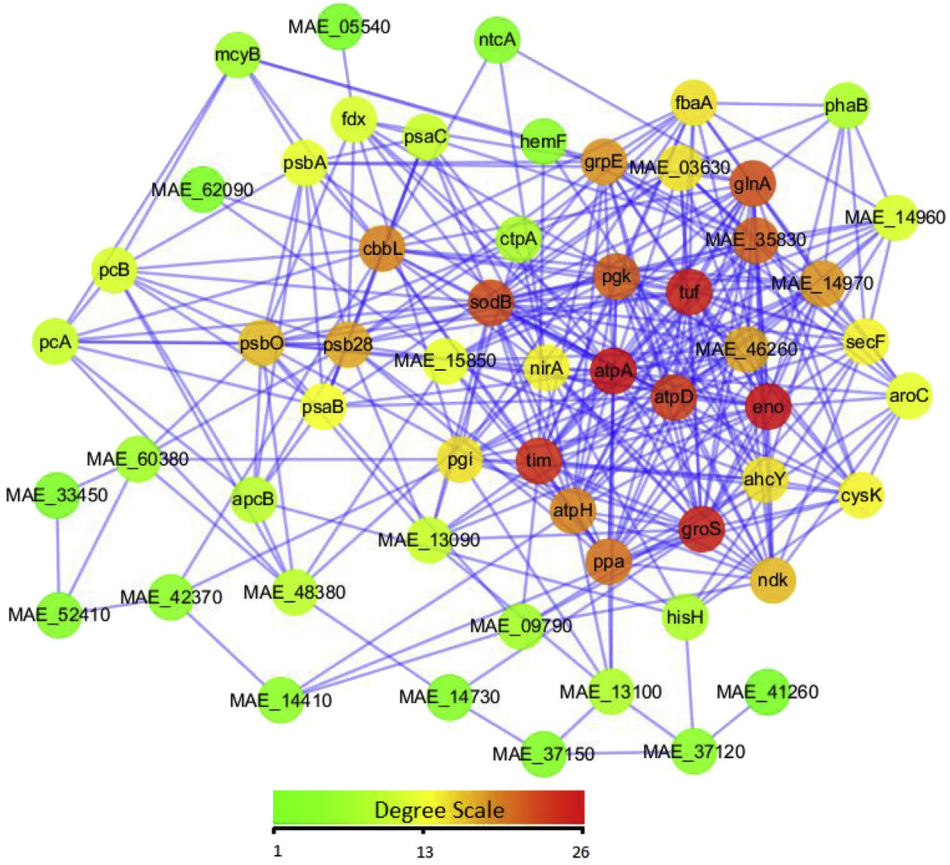

Fig. 3. The interaction network of differentially expressed proteins in *M. aeruginosa* exposed to 100 ng/L of amoxicillin for 30 days, constructed according to the STRING database. The protein symbols are shown in Table 1. The nodes are represented as circles and edges as lines. The number of edges at each node (degree) was indicated by the color. (For interpretation of the references to colour in this figure legend, the reader is referred to the web version of this article.)

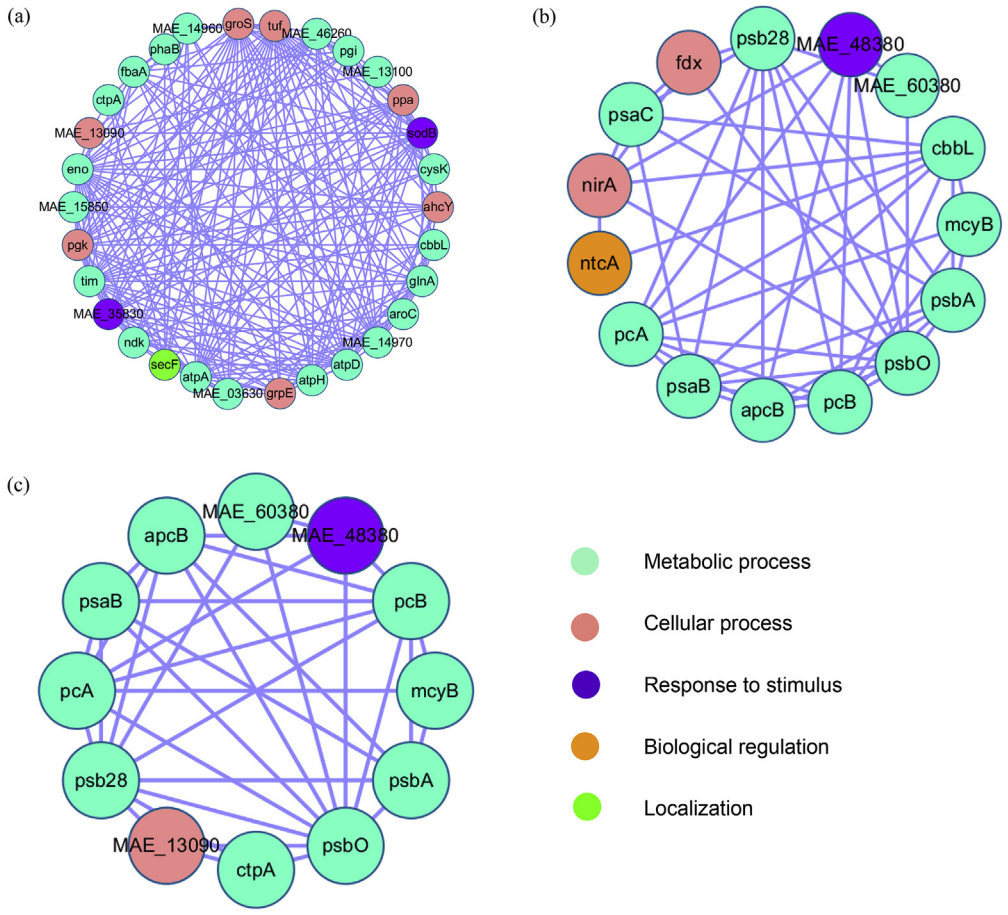

Cluster information of three protein-protein interaction modules

Cluster	Nodes	Density	In-weight	Out-weight	Quality	P value
a	30	0.503	319	68	0.763	< 0.001
b	15	0.467	59	49	0.454	0.006
c	12	0.53	49	35	0.417	0.044

Fig. 4. Three significant enriched ($p < 0.05$) protein–protein interaction modules in *M. aeruginosa* exposed to 100 ng/L of amoxicillin for 30 days based on the analysis of ClusterONE. Proteins are classified according to Gene Ontology (GO) terms of biological processes and labeled by different colors. The protein symbols are shown in Table 1. (For interpretation of the references to colour in this figure legend, the reader is referred to the web version of this article.)

metabolites and energy, electron transport chain and oxidation reduction). The two proteins are reaction centers of PSI, receive electrons from D1 protein through a electron transport chain, and transfer electrons to the carbon fixation process (Yang et al., 2015). The up-regulation of these two proteins may be induced by up-regulated D1 protein and consequently increased electron transport. Along with the up-regulation of psaB and psaC, an downstream protein essential for carbon fixation process (ccbL) was also up-regulated. The responses of the above differentially expressed proteins were in accordance with a previous study of our group, in which up-regulated expression of *psbA* gene, *psaB* gene and *ccbL* (also called *rbcL*) gene were coupled with each other in response to low concentrations of amoxicillin (Liu et al., 2015). D1 protein has been verified as the target position of several herbicides in plants and phytoplanktons, and mutation of D1 protein would lead to a low sensitivity to herbicides (Gleiter et al., 1992). Recent studies observed up-regulated expression of *psbA* gene in phytoplanktons exposed to various toxic substances (Shao et al., 2009). In this study, close correlation with other proteins and broad involvement in various biological processes suggested that D1 protein also acted as a candidate target position of amoxicillin in *M. aeruginosa*.

According to Table 3, some of the proteins were commonly shared by more than one biological process groups. Phosphoglycerate kinase, enolase, glucose-6-phosphate isomerase, fructose-bisphosphate aldolase class II, and triosephosphate isomerase were commonly shared by the photosynthesis and stress response group and the carbohydrate metabolic process group. These five proteins participate in photosynthesis, glycolysis, gluconeogenesis

and ATP generation, which were closely related with energy production and release (Kanehisa, 2013). Nucleoside diphosphate kinase and ATP synthase subunits alpha, beta and delta were commonly shared by the photosynthesis and stress response group and the nucleoside phosphate metabolic process. The three ATP synthase subunits were involved in photosynthesis and energy production, and nucleoside diphosphate kinase participate in balance control of nucleoside metabolism, signal transduction, growth regulation and stress response (Francois-Moutal et al., 2014; Rühle and Leister, 2015). Most of the above proteins were down-regulated, indicating a higher energy consumption and a lower energy storage in *M. aeruginosa* under long-term exposure to amoxicillin, compared with the control. Five of the above proteins, ATP synthase subunits alpha and beta, enolase, triosephosphate isomerase and phosphoglycerate kinase, were also among the top 10 most connective proteins in the protein–protein interaction network (Fig. 3), and were supposed to be candidate target positions of amoxicillin under long-term exposure.

The fourth biological process group in Table 2 indicated that cellular biosynthesis of *M. aeruginosa* was also affected by amoxicillin after 30 days of exposure. In this group, chorismate synthase and cysteine synthase were up-regulated, while glutamine synthetase, 3-oxoacyl-[acyl-carrier-protein] synthase II, and imidazole glycerol phosphate synthase subunit were down-regulated. This result suggested that synthesis of aromatic amino acids and cysteine was enhanced, while synthesis of glutamine, L-histidine and fatty acid were inhibited by amoxicillin (Kehr et al., 2011). The above results were in accordance with that of pathway enrichment analysis, in which carbon fixation pathway was affected by amoxicillin under long-term exposure. Energy production related proteins were also involved in this group, since biosynthesis is a energy consumption process. At last, though a highly sensitive SYPRO Ruby staining method was used to reduce the detection level of protein spots, limitation of 2-DE may still lead to missing information of some low abundant proteins. Therefore amoxicillin-induced deferentially expressed proteins in *M. aeruginosa* were supposed to be more than that observed through 2-DE. More advanced proteomic techniques involving isobaric/fluorescence labeling and liquid chromatography separation with broader proteome coverage were still required to obtain more candidate target proteins of amoxicillin.

5. Conclusions

The present study investigated the regulation effects of low test concentrations of amoxicillin on the bloom-forming cyanobacterium *M. aeruginosa* through long-term exposure. This is also the first study on the proteomic response of cyanobacteria to antibiotic contaminant. Photosynthesis was found to be the most important process in response to amoxicillin, which was closely correlated with the stimulated production of MCs and detoxification of amoxicillin. Six proteins involved in photosynthesis, glycolysis, gluconeogenesis and ATP production were found to be candidate target positions of amoxicillin in *M. aeruginosa* under long-term exposure.

Acknowledgments

This work was supported by National Natural Science Foundation of China (51209125).

Appendix A. Supplementary data

Supplementary data related to this article can be found at http://dx.doi.org/10.1016/j.watres.2016.01.060.

References

Andreani, J., Guerois, R., 2014. Evolution of protein interactions: from interactomes to interfaces. Arch. Biochem. Biophys. 554, 65–75. http://dx.doi.org/10.1016/j.abb.2014.05.010.

Babica, P., Bláha, L., Maršálek, B., 2006. Exploring the natural role of microcystins-a review of effects on photoautotrophic organisms. J. Phycol. 42 (1), 9–20. http://dx.doi.org/10.1111/j.1529-8817.2006.00176.x.

Bandow, J.E., Brötz, H., Leichert, L.I.O., Labischinski, H., Hecker, M., 2003. Proteomic approach to understanding antibiotic action. Antimicrob. Agents Chemother. 47 (3), 948–955. http://dx.doi.org/10.1128/AAC.47.3.948-955.2003.

Bangera, M., Panigrahi, R., Sagurthi, S.R., Savithri, H.S., Murthy, M.R.N., 2015. Structural and functional analysis of two universal stress proteins YdaA and YnaF from *Salmonella typhimurium*: possible roles in microbial stress tolerance. J. Struct. Biol. 189 (3), 238–250. http://dx.doi.org/10.1016/j.jsb.2015.01.003.

Castielli, O., De la Cerda, B., Navarro, J.A., Hervás, M., De la Rosa, M.A., 2009. Proteomic analyses of the response of cyanobacteria to different stress conditions. FEBS Lett. 583 (11), 1753–1758. http://dx.doi.org/10.1016/j.febslet.2009.03.069.

Chen, L.G., Sun, J., Zhang, H.M., Au, D.W.T., Lam, P.K.S., Zhang, W.P., Bajic, V.B., Qiu, J.W., Qian, P.Y., 2015. Hepatic proteomic responses in marine medaka (*Oryzias melastigma*) chronically exposed to antifouling compound butenolide [5-octylfuran-2(5H)-one] or 4,5-dichloro-2-N-Octyl-4- isothiazolin-3-One (DCOIT). Environ. Sci. Technol. 49, 1851–1859. http://dx.doi.org/10.1021/es5046748.

Dittrich, M.T., Klau, G.W., Rosenwald, A., Dandekar, T., Müller, T., 2008. Identifying functional modules in protein-protein interaction networks: an integrated exact approach. Bioinformatics 24 (13), 223–231. http://dx.doi.org/10.1093/bioinformatics/btn161.

Franc, V., Řehulka, P., Raus, M., Stulík, J., Novak, J., Renfrow, M.B., Šebela, M., 2013. Elucidating heterogeneity of IgA1 hinge-region O-glycosylation by use of MALDI-TOF/TOF mass spectrometry: role of cysteine alkylation during sample processing. J. Proteom. 92, 299–312. http://dx.doi.org/10.1016/j.jprot.2013.07.013.

Franco, D., Mato, A., Salgado, F.J., López-Pedrouso, M., Carrera, M., Bravo, S., Parrado, M., Gallardo, J.M., Zapata, C., 2015. Tackling proteome changes in the l*ongissimus thoracis* bovine muscle in response to pre-slaughter stress. J. Proteom. 122, 73–85. http://dx.doi.org/10.1016/j.jprot.2015.03.029.

Francois-Moutal, L., Marcillat, O., Granjon, T., 2014. Structural comparison of highly similar nucleoside-diphosphate kinases: molecular explanation of distinct membrane-binding behavior. Biochimie 105, 110–118. http://dx.doi.org/10.1016/j.biochi.2014.06.025.

Gleiter, H.M., Ohad, N., Koike, H., Hirschberg, J., Renger, G., Inoue, Y., 1992. Thermoluminescence and flash-induced oxygen yield in herbicide resistant mutants of the D1 protein in *Synechococcus* PCC7942. Biochim. Biophys. Acta Bioenerg. 1140 (2), 135–143. http://dx.doi.org/10.1016/0005-2728(92)90002-J.

González-Pleiter, M., Gonzalo, S., Rodea-Palomares, I., Leganés, F., Rosal, R., Boltes, K., Marco, E., Fernández-Piñas, F., 2013. Toxicity of five antibiotics and their mixtures towards photosynthetic aquatic organisms: implications for environmental risk assessment. Water Res. 47 (6), 2050–2064. http://dx.doi.org/10.1016/j.watres.2013.01.020.

Graham, J.L., Loetin, K.A., Meyer, M.T., Ziegler, A.C., 2010. Cyanotoxin mixtures and taste-and-odor compounds in cyanobacterial blooms from the Midwestern United States. Environ. Sci. Technol. 44 (19), 7361–7368. http://dx.doi.org/10.1021/es1008938.

Guarino, C., Conte, B., Spada, V., Arena, S., Sciarrillo, R., Scaloni, A., 2014. Proteomic analysis of eucalyptus leaves unveils putative mechanisms involved in the plant response to a real condition of soil contamination by multiple heavy metals in the presence or absence of mycorrhizal/rhizobacterial additives. Environ. Sci. Technol. 48, 11487–11496. http://dx.doi.org/10.1021/es502070m.

Gupta, N., Pant, S.C., Vijayaraghavan, R., Rao, P.V., 2003. Comparative toxicity evaluation of cyanobacterial cyclic peptide toxin microcystin variants (LR, RR,YR) in mice. Toxicology 188 (2–3), 285–296. http://dx.doi.org/10.1016/S0300-483X(03)00112-4.

Halling-Sørensen, B., 2000. Algal toxicity of antibacterial agents used in intensive farming. Chemosphere 40 (7), 731–739. http://dx.doi.org/10.1016/S0045-6535(99)00445-2.

He, J., Han, G.Y., Chen, D.W., 2013. Insights into enzyme secretion by filamentous fungi: comparative proteome analysis of *Trichoderma reesei* grown on different carbon sources. J. Proteom. 89, 191–201. http://dx.doi.org/10.1016/j.jprot.2013.06.014.

Hiriart-Baer, V.P., Fortin, C., Lee, D.Y., Campbell, P.G.C., 2006. Toxicity of silver to two freshwater algae, *Chlamydomonas reinhardtii* and *Pseudokirchneriella subcapitata*, grown under continuous culture conditions: influence of thiosulphate. Aquat. Toxicol. 78 (2), 136–148. http://dx.doi.org/10.1016/j.aquatox.2006.02.027.

Horii, T., Mase, K., Suzuki, Y., Kimura, T., Ohta, M., Maekawa, M., Kanno, T., Kobayashi, M., 2002. Antibacterial activities of beta-lactamase inhibitors associated with morphological changes of cell wall in Helicobacter pylori. Helicobacter 7, 39–45. http://dx.doi.org/10.1046/j.1523-5378.2002.00054.x.

Huang, D.W., Sherman, B.T., Lempicki, R.A., 2009a. Systematic and integrative analysis of large gene lists using DAVID bioinformatics resources. Nat. Protoc. 4 (1), 44–57. http://dx.doi.org/10.1038/nprot.2008.211.

Huang, D.W., Sherman, B.T., Lempicki, R.A., 2009b. Bioinformatics enrichment tools: paths toward the comprehensive functional analysis of large gene lists. Nucleic

Acids Res. 37 (1), 1–13. http://dx.doi.org/10.1093/nar/gkn923.
Kanehisa, M., 2013. Chemical and genomic evolution of enzyme-catalyzed reaction networks. FEBS Lett. 587 (17), 2731–2737. http://dx.doi.org/10.1016/j.febslet.2013.06.026.
Kehr, J.C., Gatte Picchi, D., Dittmann, E., 2011. Natural product biosyntheses in cyanobacteria: a treasure trove of unique enzymes. Beilstein J. Org. Chem. 7, 1622–1635. http://dx.doi.org/10.1016/j.febslet.2013.06.026.
Kümmerer, K., 2009. Antibiotics in the aquatic environment-a review-Part I. Chemosphere 75 (4), 417–434. http://dx.doi.org/10.1016/j.chemosphere.2008.11.086.
Liu, Y., Chen, X., Zhang, J., Gao, B.Y., 2015. Hormesis effects of amoxicillin on growth and cellular biosynthesis of *Microcystis aeruginosa* at different nitrogen levels. Microb. Ecol. 69 (3), 608–617. http://dx.doi.org/10.1007/s00248-014-0528-9.
Liu, Y., Gao, B.Y., Yue, Q.Y., Guan, Y.T., Wang, Y., Huang, L.H., 2012. Influences of two antibiotic contaminants on the production, release and toxicity of microcystins. Ecotoxicol. Environ. Saf. 77, 79–87. http://dx.doi.org/10.1016/j.ecoenv.2011.10.027.
Mehta, A., López-Maury, L., Florencio, F.J., 2014. Proteomic pattern alterations of the cyanobacterium *Synechocystis* sp. PCC 6803 in response to cadmium, nickel and cobalt. J. Proteom. 102, 98–112. http://dx.doi.org/10.1016/j.jprot.2014.03.002.
Migliore, L., Godeas, F., De Filippis, S.P., Mantovi, P., Barchi, D., Testa, C., Rubattu, N., Brambilla, G., 2010. Hormetic effect(s) of tetracyclines as environmental contaminant on Zea mays. Environ. Pollut. 158 (1), 129–134. http://dx.doi.org/10.1016/j.envpol.2009.07.039.
Ni, L.X., Jie, X.T., Wang, P.F., Li, S.Y., Wang, G.X., Li, Y.P., Li, Y., Acharya, K., 2015. Effect of linoleic acid sustained-release microspheres on *Microcystis aeruginosa* antioxidant enzymes activity and microcystins production and release. Chemosphere 121, 110–116. http://dx.doi.org/10.1016/j.chemosphere.2014.11.056.
Pomati, F., Netting, A.G., Calamari, D., Neilan, B.A., 2004. Effects of erythromycin, tetracycline and ibuprofen on the growth of *Synechocystis* sp. and *Lemna minor*. Aquat. Toxicol. 67 (4), 387–396. http://dx.doi.org/10.1016/j.aquatox.2004.02.001.
Pruden, A., 2014. Balancing water sustainability and public health goals in the face of growing concerns about antibiotic resistance. Environ. Sci. Technol. 48 (1), 5–14. http://dx.doi.org/10.1021/es403883p.
Pumirat, P., Saetun, P., Sinchaikul, S., Chen, S.T., Korbsrisate, S., Thongboonkerd, V., 2009. Altered secretome of *Burkholderia pseudomallei* induced by salt stress. Biochim. Biophys. Acta Proteins Proteom. 1794 (6), 898–904. http://dx.doi.org/10.1016/j.bbapap.2009.01.011.
Qian, H.F., Pan, X.J., Chen, J., Zhou, D.M., Chen, Z.G., Zhang, L., Fu, Z.W., 2012. Analyses of gene expression and physiological changes in *Microcystis aeruginosa* reveal the phytotoxicities of three environmental pollutants. Ecotoxicology 21 (3), 847–859. http://dx.doi.org/10.1007/s10646-011-0845-4.
Rodriguez-Mozaz, S., Chamorro, S., Marti, E., Huerta, B., Gros, M., Sànchez-Melsió, A., Borrego, C.M., Barceló, D., Balcázar, J.L., 2015. Occurrence of antibiotics and antibiotic resistance genes in hospital and urban wastewaters and their impact on the receiving river. Water Res. 69, 234–242. http://dx.doi.org/10.1016/j.watres.2014.11.021.
Rühle, T., Leister, D., 2015. Assembly of F1F0-ATP synthases. Biochim. Biophys. Acta Bioenerg. 1847 (9), 849–860. http://dx.doi.org/10.1016/j.bbabio.2015.02.005.
Shao, J.H., Wu, Z.X., Yu, G.L., Peng, X., Li, R.H., 2009. Allelopathic mechanism of pyrogallol to *Microcystis aeruginosa* PCC7806 (Cyanobacteria): from views of gene expression and antioxidant system. Chemosphere 75 (7), 924–928. http://dx.doi.org/10.1016/j.chemosphere.2009.01.021.
Stanier, R.Y., Cohen-Bazire, G., 1977. Phototrophic prokaryotes: the cyanobacteria. Annu. Rev. Microbiol. 31, 225–274. http://dx.doi.org/10.1146/annurev.mi.31.100177.001301.
Wan, J., Guo, P., Peng, X.F., Wen, K.Q., 2015. Effect of erythromycin exposure on the growth, antioxidant system and photosynthesis of *Microcystis flos-aquae*. J. Hazard. Mater. 283, 778–786. http://dx.doi.org/10.1016/j.jhazmat.2014.10.026.
Wang, Z.C., Li, D.H., Li, G.W., Liu, Y.D., 2010. Mechanism of photosynthetic response in *Microcystis aeruginosa* PCC7806 to low inorganic phosphorus. Harmful Algae 9, 613–619. http://dx.doi.org/10.1016/j.hal.2010.04.012.
Yang, H.X., Liu, J., Wen, X.G., Lu, C.M., 2015. Molecular mechanism of photosystem I assembly in oxygenic organisms. Biochim. Biophys. Acta Bioenerg. 847 (9), 838–848. http://dx.doi.org/10.1016/j.bbabio.2014.12.011.
Zhang, D.X., Yan, H., Hu, J.Y., Zhang, J.P., Teng, M., Tong, D.L., Xiang, F., Zhang, Q., Fang, Y.D., Liang, G.P., Huang, Y.S., 2012. Identification of mitochondria translation elongation factor Tu as a contributor to oxidative damage of postburn myocardium. J. Proteom. 77, 469–479. http://dx.doi.org/10.1016/j.jprot.2012.09.024.
Zuccato, E., Castiglioni, S., Bagnati, R., Melis, M., Fanelli, R., 2010. Source, occurrence and fate of antibiotics in the Italian aquatic environment. J. Hazard. Mater. 179 (1–3), 1042–1048. http://dx.doi.org/10.1016/j.jhazmat.2010.03.110.